Polarized mm And sub-mm Emission From Sgr A* At The Galactic Center

Fulvio Meli $a^{\dagger 1}$
† Physics Department and Steward Observatory, The University of Arizona, Tucson, AZ 8572
Siming Liu^*
*Physics Department, The University of Arizona, Tucson, AZ 85721 $$
and
Robert Coker [‡]
$^{\ddagger} \mathrm{Department}$ of Physics & Astronomy, The University of Leeds, Leeds LS2 9JT, UK

 ${\it accepted} \; _$

 $^{^1\}mathrm{Sir}$ Thomas Lyle Fellow and Miegunyah Fellow.

ABSTRACT

The recent detection of significant linear polarization at mm and sub-mm wavelengths in the spectrum of Sgr A* (if confirmed) will be a useful probe of the conditions within several Schwarzschild radii (r_S) of the event horizon at the Galactic Center. Hydrodynamic simulations of gas flowing in the vicinity of this object suggest that the infalling gas circularizes when it approaches within $5-25 r_S$ of the black hole. We suggest that the sub-mm "excess" of emission seen in the spectrum of Sgr A* may be associated with radiation produced within the inner Keplerian region and that the observed polarization characteristics provide direct evidence for this phenomenon. The overall spectrum from this region, including the high-energy component due to bremsstrahlung and inverse Compton scattering processes, is at or below the recent Chandra measurement, and may account for the X-ray source if it turns out to be the actual counterpart to Sgr A*.

Subject headings: accretion—black hole physics—hydrodynamics—Galaxy: center—magnetic fields: dynamo—radiation: polarization

1. INTRODUCTION

Discovered over 25 years ago (Balick & Brown 1974), Sgr A* is a bright, compact radio source coincident with the dynamical center of the Galaxy, and now provides possibly the most compelling evidence for the existence of supermassive black holes. The suggested central dark mass concentration within the inner 0.015 pc of the Galactic center is $2.6 \pm 0.2 \times 10^6 M_{\odot}$ (Genzel et al. 1996; Eckart & Genzel 1996; Eckart & Genzel 1997; Ghez et al. 1998). (0.1" corresponds to 800 Astronomical Units, or roughly 1.2×10^{16} cm at a distance of 8.5 kpc.) Most of this mass is probably associated with Sgr A*.

The spectrum of this unusual object is seen to be bumpy, but can be described as a power-law with a spectral index a that varies between roughly 0.19 - 0.34 ($S_{\nu} \propto \nu^{a}$) between GHz and mm wavelengths. However, one of the most interesting features currently under focus is the suggestion of a sub-millimeter (sub-mm) bump in the spectrum (Zylka et al. 1992; Zylka et al. 1995), since in all emission models the highest frequencies correspond to the smallest spatial scales, so that the sub-millimeter emission comes directly from the vicinity of the black hole (Melia 1992, 1994; Melia, Jokipii & Narayanan 1992; Coker and Melia 2000). The existence of this bump (or "excess") has been uncertain due to the variability of Sgr A*, but is now well established following a set of simultaneous observations (from $\lambda 20$ cm to $\lambda 1$ mm) using the VLA, BIMA, Nobeyama 45 m, & IRAM 30 m telescopes (Falcke, et al. 1998).

More recently, radio observations of Sgr A* have focused on the detection of polarization from this source. Although the upper limits to the linear polarization in Sgr A* are found to be quite low (less than 1%) below 86 GHz (Bower et al. 1999), this is not the case at 750, 850, 1350, and 2000 μ m, where a surprisingly large intrinsic polarization of over 10% has now been reported (Aitken, et al. 2000). ¿From the lack of polarization at longer wavelengths, Aitken et al. conclude that their measured values at higher frequencies must arise in the mm/sub-mm "excess". These observations also point to the tantalizing result that the position angle changes considerably (by about 80°) between the mm and the sub-mm portions of the spectrum, which one would think must surely have something to do with the fact that the emitting gas becomes transparent at sub-mm wavelengths (Melia 1992, 1994).

In a companion paper (Melia, Liu & Coker 2001) we suggested that the mm and sub-mm "excess" in the spectrum of Sgr A* may be the first indirect evidence for the anticipated circularization of the gas falling into the black hole at $5-25 r_S$, where $r_S \equiv 2GM/c^2$ is the Schwarzschild radius. The abundance of gas in the environment surrounding Sgr A* clearly points to accretion as the incipient cause of the ensuing energetic behavior of this source (Melia 1994)—whether or not it eventually leads to expulsion of

some plasma at smaller radii (see, e.g., Falcke et al. 1993). In their simulation of the Bondi-Hoyle accretion onto Sgr A* from the surrounding winds, Coker & Melia (1997) concluded the accreted specific angular momentum $l \equiv \lambda r_S c$ can vary by 50% over $\lesssim 200$ years with an average equilibrium value in λ of about 30 or less. Although this shows that relatively little specific angular momentum is accreted—so that large disks (such as those required in ADAF models; Narayan et al. 1996) probably do not form around Sgr A*—it does nonetheless lead to the expectation that the plasma must circularize toward smaller radii before flowing through the event horizon. However, given the fluctuations in the accreted value of λ (both in magnitude and sign!), this Keplerian flow is variable, and it probably dissolves and reforms (possibly with a different sense of spin) on a time scale of ~ 100 years or less.

Melia et al. (2001) demonstrated how this dichotomy comprising a quasi-spherical flow at radii beyond $50 r_S$ or so, and a Keplerian structure toward smaller radii, may be the explanation for Sgr A*'s spectrum, including the appearance of the "excess", which is viewed as arising primarily within the circularized component. It is our intention in this *Letter* to demonstrate how the linear polarization data may now be taken as direct evidence for the existence of this accretion profile.

2. METHODOLOGY

The structure of the flow within the circularization radius (at $\sim 5-50~r_S$) is developed fully in Melia et al. (2001). For the sake of completeness, we highlight the key elements of this calculation below. Central to the modeling of the sub-mm "excess" is the supposition that within the Keplerian flow, a magnetohydrodynamic dynamo produces an enhanced (though still sub-equipartition) magnetic field, dominated by its azimuthal component (Hawley, Gammie & Balbus 1996). Although the process of magnetic field dissipation suppresses the field intensity well below its equipartition value in the quasi-spherical region (Kowalenko & Melia 2000), the magnetic dynamo evidently overwhelms the rate of field destruction in the differentially rotating portion of the inflow, and the field reaches a saturated intensity. The sub-mm "excess" in Sgr A* may be the thermal synchrotron radiation produced in this inner region.

At a (cylindrical) radius r in the Keplerian flow where the column density is Σ and the angular velocity is $\Omega = (GM/r^3)^{1/2}$, the radial velocity is given as (e.g., Stoeger 1980)

$$v_r = -\frac{3}{r^{1/2}\Sigma} \frac{\partial}{\partial r} \left(\nu \Sigma r^{1/2} \right) , \qquad (1)$$

where $\nu = (2/3)W_{r\phi}/\Sigma \Omega$ is the kinematic viscosity, and $W_{r\phi}$ is the vertically integrated sum of the Maxwell

and Reynolds stresses (Balbus et al. 1994). For the problem at hand, the Maxwell stress dominates, and

$$W_{r\phi} \approx \beta_{\nu} \int dz \, \langle \frac{B^2}{8\pi} \rangle \,,$$
 (2)

where B is the turbulent magnetic field (the average inside the integral being taken over time). Numerical simulations (e.g., by Brandenburg et al. 1995) show that β_{ν} changes very slowly with r. In the particular cases considered by these authors, β_{ν} ranged in value from ≈ 0.1 to 0.2, while r decreased by a factor of 5. For simplicity, we will here adopt a "mean" value of ~ 0.15 for this quantity.

For steady conditions, one can obtain the vertical profile by assuming that the gas is in local hydrostatic equilibrium. Balancing gravity and the pressure gradient in the vertical direction, we obtain the scale height $H = \sqrt{2R_gTr^3/\mu GM}$, where T is the gas temperature at radius r, R_g is the gas constant, and μ is the molecular weight. For simplicity, we will assume that the Keplerian flow is axisymmetric and is independent of the vertical coordinate. Written another way, we have $(H\Omega)^2 = 2P/\rho$, where P is the gas pressure and ρ is the mass density of the gas. The numerical simulations of the magnetohydrodynamic dynamo effect indicate that the field intensity is somewhat below its equipartition value, so that

$$\int dz \, \langle \frac{B^2}{8\pi} \rangle \approx \beta_p \int P \, dz = \beta_p \frac{R_g \Sigma T}{\mu} \,, \tag{3}$$

where β_p is roughly constant with a value of ≈ 0.02 . Thus, with $\dot{M} = -2\pi r \Sigma v_r$, we can integrate Equation (1) to obtain v_r , and T follows directly from the energy conservation equation (Melia et al 2001).

3. CALCULATION OF THE SPECTRUM

The flux density (at earth) produced by the Keplerian portion of the flow is given by

$$F_{\nu_0} = \frac{1}{D^2} \int I_{\nu'} \sqrt{1 - r_S/r} \, dA \,, \tag{4}$$

where D=8.5 kpc is the distance to the Galactic Center, ν_0 is the observed frequency at infinity and ν' is the frequency measured by a stationary observer in the Schwarzschild frame. (For simplicity, we here assume the metric for a non-spinning black hole. A more thorough exploration of the parameter values, including the black hole spin, will be discussed elsewhere.) The frequency transformations are given by

$$\nu_0 = \nu' \sqrt{1 - r_S/r} , \qquad \nu' = \nu \frac{\sqrt{1 - v_\phi^2/c^2}}{1 - (v_\phi/c)\cos\theta} ,$$
 (5)

where ν is the frequency measured in the co-moving frame, and θ is the angle between the velocity \vec{v}_{ϕ} and the line of sight. Since the radial velocity is always much smaller than v_{ϕ} , we ignore this component

in the transformation equations. So $\cos\theta = \sin i \, \cos\phi$, where i is the inclination angle of the axis perpendicular to the Keplerian flow, and ϕ is the azimuth of the emitting element. When the Doppler shift is included, the blue shifted region is located primarily near $\phi = 0$ while the red shifted region is at $\phi = \pi$. The other quantities that are necessary for an evaluation of the flux density are the area element $dA = \sqrt{1 - r_S/r}^{-1} \cos i \, r \, dr \, d\phi$, and the specific intensity $I_{\nu'} = B'_{\nu'} (1 - e^{-\tau})$, where

$$B'_{\nu'} = \left(\frac{\sqrt{1 - v_{\phi}^2/c^2}}{1 - (v_{\phi}/c)\cos\theta}\right)^3 B_{\nu} , \qquad (6)$$

and the optical depth is

$$\tau = \int \kappa'_{\nu'} ds = \kappa_{\nu} \frac{2H}{\cos i} \frac{1 - (v_{\phi}/c)\cos\theta}{\sqrt{1 - v_{\phi}^2/c^2}},$$
 (7)

where κ_{ν} is the absorption coefficient. When $\tau \ll 1$, Kirchoff's law allows us to write

$$I_{\nu'} \approx B'_{\nu'} \tau = \epsilon_{\nu} \frac{2H}{\cos i} \left(\frac{\sqrt{1 - v_{\phi}^2/c^2}}{1 - (v_{\phi}/c)\cos \theta} \right)^2 ,$$
 (8)

where $\epsilon_{\nu} = B_{\nu} \kappa_{\nu}$ is the emissivity.

The presence of a substantial azimuthal component of the magnetic field makes it convenient to calculate the observed flux directly from the Extraordinary and Ordinary components of the intensity. The most convenient approach is to select the symmetry axis of the Keplerian flow as the reference direction. The observed flux densities in the azimuthal and the reference directions are given by

$$F_{1\nu_0} = \frac{1}{D^2} \int (I_{\nu'}^e \cos^2 \phi' + I_{\nu'}^o \sin^2 \phi') \sqrt{1 - r_S/r} \, dA , \qquad (9)$$

$$F_{2\nu_0} = \frac{1}{D^2} \int (I_{\nu'}^e \sin^2 \phi' + I_{\nu'}^o \cos^2 \phi') \sqrt{1 - r_S/r} \, dA , \qquad (10)$$

respectively, where $\phi' + \pi/2$ is the position angle of the magnetic field vector within the emitting element that has an azimuth of ϕ , so that $\cot \phi' = \cot \phi \cos i$. $I^e_{\nu'}$ and $I^o_{\nu'}$ are the specific intensities for the Extraordinary and Ordinary waves, respectively. For thermal synchrotron radiation, the emissivities are

$$\epsilon^e = \frac{\sqrt{3}e^3}{8\pi m_e c^2} B \sin \theta' \int_0^\infty N(E) [F(x) + G(x)] dE,$$
(11)

$$\epsilon^{o} = \frac{\sqrt{3}e^{3}}{8\pi m_{e}c^{2}}B\sin\theta' \int_{0}^{\infty} N(E)[F(x) - G(x)] dE,$$
(12)

where N(E) is the electron distribution function at energy E, and

$$\cos \theta' = \frac{\cos \theta - v_{\phi}/c}{1 - (v_{\phi}/c)\cos \theta}, \qquad x = \frac{4\pi \nu m_e^3 c^5}{3eB \sin \theta' E^2}, \qquad (13)$$

$$F(x) = x \int_{x}^{\infty} K_{5/3}(z) dz$$
, $G(x) = x K_{2/3}(x)$. (14)

 $K_{5/3}$ and $K_{2/3}$ are the corresponding modified Bessel functions (Pacholczyk 1970). The total flux density produced by the Keplerian portion of the flow is the sum of these two. The expected fractional polarization is then given by $P_{\nu_0} = (F_{1\nu_0} - F_{2\nu_0})/(F_{1\nu_0} + F_{2\nu_0})$.

The temperature in this region reaches $\sim 10^{11}$ K, for which inverse Compton processes must be taken into account. The self-Comptonization of the sub-mm radiation is calculated according to the prescription in Melia et al. (2001), based on the algorithm described in Melia & Fatuzzo (1989).

4. RESULTS AND CONCLUSIONS

The best-fit model for the polarized mm and sub-mm emission from Sgr A* (Aitken et al. 2000) is shown in Figures 1 (the inset) and (the solid curve of) 2. The peak frequency of the flux density is 2.4×10^{11} Hz, and the flip frequency (at which the position angle changes by 90°) is 2.8×10^{11} Hz. Below this frequency, the first component is smaller than the second, and the corresponding percentage polarization is therefore (by definition) negative. Above the flip frequency, the first component is larger. Although the fit is not optimized, both the spectrum and the percentage polarization appear to be consistent with the data. It is to be noted that the peak frequency is actually *smaller* than the flip frequency, which is distinct from other models that may also produce a rotation of the position angle (see Aitken et al. 2000).

It is rather straightforward to understand the polarization characteristics in this model. In the optically thick region (below about 1.6×10^{11} Hz), the specific intensity of the Extraordinary and Ordinary waves is almost isotropic in the co-moving frame because the optical depth τ is very large. Even with the inclusion of the Doppler effect, the emissivity of the source is relatively independent of position angle. But the optical depths are different for the two waves, as indicated by Equation (7), and the specific intensity of the Extraordinary wave is slightly larger than that of the Ordinary wave. From Equations (11) and (12), we see that the second component is larger than the first, and the percentage polarization is therefore negative according to the definition of P_{ν_0} . With an increase in frequency, the Extraordinary amplitude becomes even larger (relative to that of the Ordinary wave) and so the percentage polarization increases.

However, in the optically thin region, the specific intensity is given by Equation (8). The synchrotron emissivity is very sensitive to the angle between the line of sight and the magnetic field vector \mathbf{B} ; synchrotron radiation is beamed into a plane perpendicular to \mathbf{B} in the co-moving frame. With the inclusion of the Doppler effect, the radiation is beamed into a cone, and the dominant contribution comes from the blue

shifted region which has an azimuth of about zero. Therefore, since the Extraordinary wave is more intense than the Ordinary wave and the integrals (11) and (12) are dominated by radiation from the emitting element with an azimuth of about zero, the first component is larger than the second. In this case, the fractional polarization becomes positive.

In other words, the optically thick emission is dominated by emitting elements on the near and far sides of the black hole, for which the Extraordinary wave has a polarization direction parallel to the reference axis. In contrast, the dominant contribution in the thin region comes from the blue shifted emitter to the side of the black hole, where the Extraordinary wave has a polarization direction mostly perpendicular to this axis. The sharp decrease in polarization at still higher frequencies is due to the diluting effects of Comptonization emission which begins to dominate over Synchrotron emission at that point. The inclination angle dependence of the fractional polarization associated with emission by the Keplerian portion of the inflow is shown in Figure 2.

Several issues remain to be investigated. An important result of our analysis is that only modest accretion rates appear to be consistent with the polarization characteristics of Sgr A* at mm and sub-mm wavelengths. The emitting region is compact—evidently no larger than a handful of Schwarzschild radii. Yet hydrodynamical simulations (Coker & Melia 1997) suggest that the rate at which plasma is captured at larger radii (of order $10^4 r_S$ or so) is several orders of magnitude higher. If our modeling is correct, this would seem to suggest that \dot{M} is variable, perhaps due to a gradual loss of mass with decreasing radius (see, e.g., Blandford & Begelman 1999). It is essential to self-consistently match the conditions within the Keplerian region of the flow with the quasi-spherical infall further out. These calculations are currently under way, and the results will be reported elsewhere. In addition, if the *Chandra* source is indeed the counterpart to Sgr A* (Baganoff et al 2000), then the spectrum shown in Figure 1 suggests a correlated variability between the sub-mm and X-ray fluxes, which can be tested with the next round of coordinated observations.

5. ACKNOWLEDGMENTS

We are very grateful to Marco Fatuzzo for helpful discussions. This work was supported by a Sir Thomas Lyle Fellowship and a Miegunyah Fellowship for distinguished overseas visitors at the University of Melbourne, and by NASA grants NAG5-8239 and NAG5-9205.

REFERENCES

Aitken, DK., Greaves, J., Chrysostomou, A., Jenness, T., Holland, W., Hough, JH., Pierce-Price, D. & Richer, J. 2000, ApJ Letters, 534, 173

Baganoff, R., et al. 2000, ApJ, to be submitted

Balbus, SA., Gammie, CF. & Hawley, JF. 1994, MNRAS, 271, 197

Balick, B. & Brown, RL 1974, ApJ, 194, 265

Blandford, RD & Begelman, RC 1999, MNRAS, 303L, 1

Bower, GC., Wright, MCH., Backer, DC. & Falcke, H. 1999, ApJ, 527, 851

Brandenburg, A., Nordlund, AA. Stein, R. & Torkelsson, U. 1995, ApJ, 446, 741

Coker, R. & Melia, F. 1997, ApJ Letters, 488, 149

Coker, R. & Melia, F. 2000, ApJ, 534, 723

Eckart, A. & Genzel, R. 1996, Nature, 383, 415

Eckart, A. & Genzel, R. 1997, MNRAS, 284, 576

Falcke, H., Mannheim, K. & Biermann, PL. 1993, AA, 278, L1

Falcke, H., Goss, WM., Matsuo, H., Teuben, P., Zhao, J-H & Zylka, R. 1998, ApJ, 499, 731

Genzel, R., Thatte, N., Krabbe, A., Kroker, H. & Tacconi-Garman, LE. 1996, ApJ, 472, 153

Ghez, AM., Klein, BL., Morris, M. & Becklin, EE. 1998, ApJ, 509, 678

Hawley, JF., Gammie, CF., Balbus, SA. 1996, ApJ, 464, 690

Kowalenko, V, & Melia, F. 2000, MNRAS, 310, 1053

Melia, F. 1992, ApJ Letters, 387, 25

Melia, F. 1994, ApJ, 426, 577

Melia, F. & Fatuzzo, M. 1989, ApJ, 346, 378

Melia, F., Liu, S. & Coker, RF. 2001, ApJ, in press

Melia, F., Jokipii, JR. & Narayanan, A. 1992, ApJ Letters, 395, 87

Narayan, R., Yi, I. & Mahadevan, R. 1996, AAS, 120, 287

Pacholczyk, AG. 1970, Radio Astrophysics, (W.H. Freeman and Company: San Francisco)

Stoeger, WR. 1980, ApJ, 235, 216

Zylka, R., Mezger, PG. & Lesch, H. 1992, AA, 261, 119

Zylka, R., Mezger, PG., Ward-Thompson, D., Duschl, WJ. & Lesch, H. 1995, AA, 297, 83

This manuscript was prepared with the AAS $\mbox{\sc IAT}_{\mbox{\sc E}}\mbox{\sc X}$ macros v4.0.

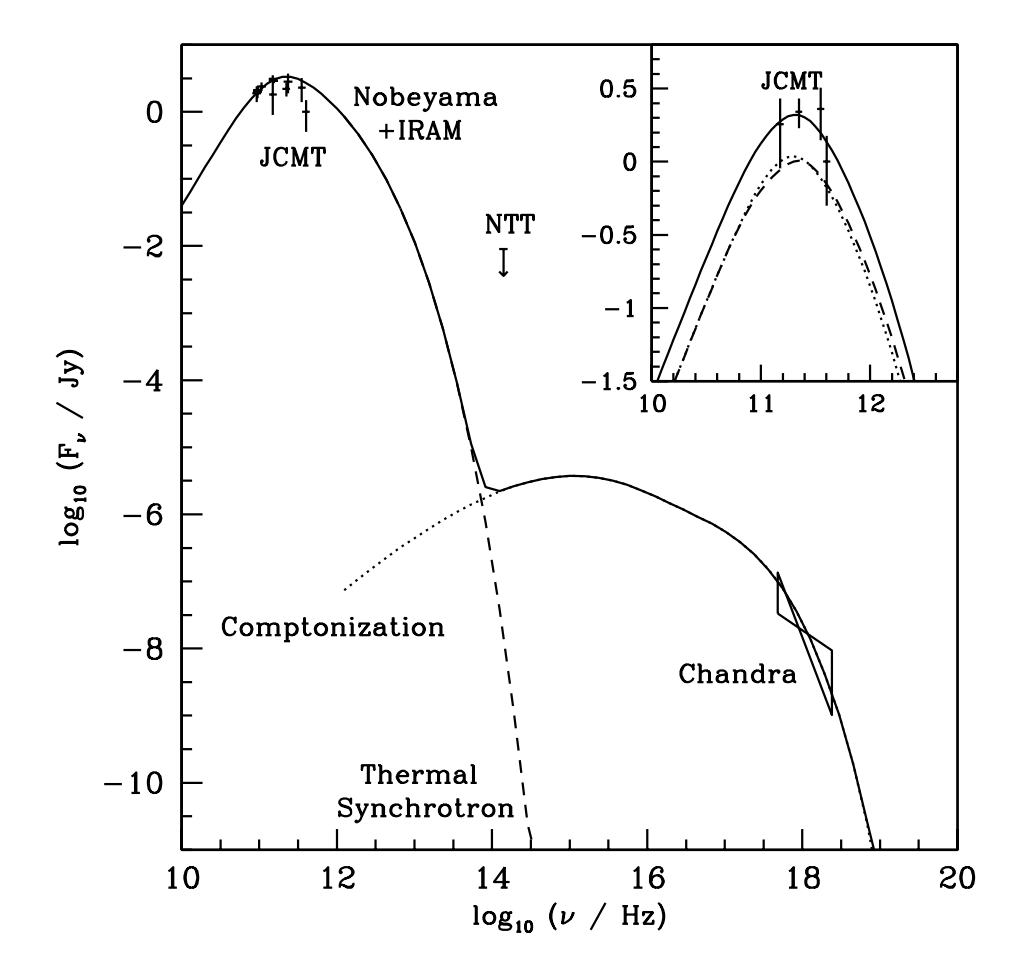


Fig. 1.— The overall spectrum from this region (optimized to fit the Nobeyama and IRAM data; Falcke et al. 1998) is shown in the main portion of this figure. Dashed: thermal synchrotron, dotted: self-Comptonization, solid: total spectrum. The bremsstrahlung emission is negligible on this scale. The parameter values are $\dot{M}=1\times 10^{16}~{\rm g~s^{-1}},~\beta_p=0.036,~\beta_\nu=0.27,~r_i=1.0~r_S$ and $r_0=5.0~r_S$. The inclination angle of the axis perpendicular to the Keplerian plane is $i=60^{\circ}$. It is also necessary to specify the ratio of v_r to its free-fall value at r_0 . For this model, this ratio is 5.0×10^{-5} . The mm to sub-mm spectrum corresponding to the best fit model for the JCMT data (which were obtained 3 years after the Nobeyama plus IRAM observations) is shown in the inset. The dotted curve corresponds to the first component and the dashed curve corresponds to the second component. The solid curve is the sum of these two. Here, $\dot{M}=4.0\times 10^{15}~{\rm g~s^{-1}},~\beta_p=0.02,$ $\beta_\nu=0.15,~r_i=1.0~r_S,~r_0=4.0~r_S$ and $i=45^{\circ}$. The ratio of velocities at r_0 is 4.0×10^{-5} .

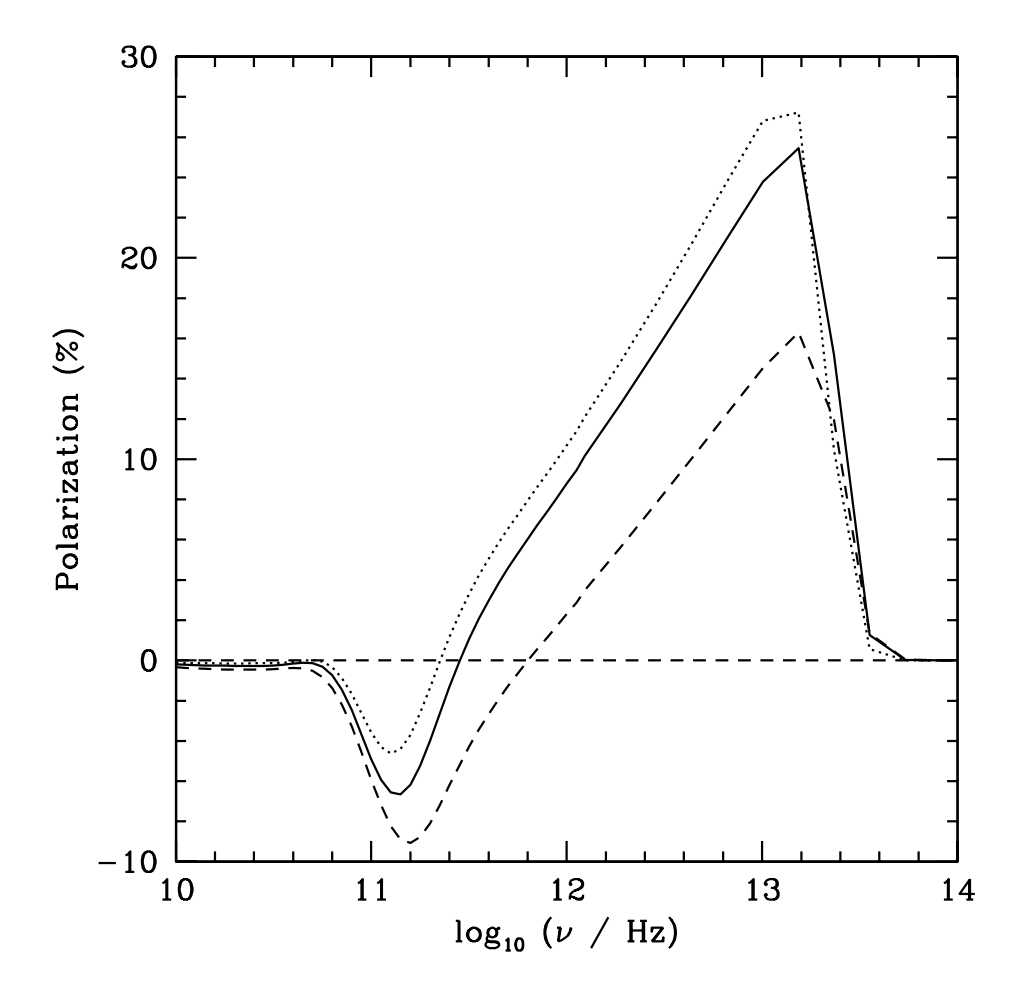


Fig. 2.— The percentage polarization for the best fit model whose spectrum is shown in the inset of Fig. 1 is here indicated by the solid curve ($i = 45^{\circ}$). The inclination angle dependence of this quantity is illustrated by the curves corresponding to an inclination angle $i = 35^{\circ}$ (dotted), and $i = 55^{\circ}$ (dashed).